Feature Article

Single Image Restoration for Participating Media Based on Prior Fusion

Joel Felipe de Oliveira Gaya
Universidade Federal do Rio Grande

Amanda Duarte
Universidade Federal do Rio Grande

Felipe Codevilla Moraes
Universidade Federal do Rio Grande
Centre de Visió per Computador

Paulo Drews-Jr
Universidade Federal do Rio Grande

Silvia Silva da Costa Botelho
Universidade Federal do Rio Grande

***Abstract*—This paper describes a method to restore degraded images captured in a participating media—fog, turbid water, sand storm, etc. Differently from the related work that deals with each medium separately, we obtain generality by using an image formation model and a fusion of new image priors.**

A PARTICIPATING MEDIUM is composed of many particles in suspension that affect the image formation. Some examples of this medium is underwater medium, fog, sand storm, etc. Images taken in such environments are degraded due the interaction between the light and the particles. This degradation occurs because the light rays interact with the medium being scattered and absorbed producing information loss. Furthermore, particles outside the field of view scatter over the image generating a characteristic veil reducing the image contrast.

Most of the restoration methods for images acquired in participating medium rely on a physical image formation model. This model describes a linear superposition between the signal and the veil. Usually, restoration methods estimate: (i) the properties of the veil, also named *veiling light*, and (ii) the properties of the medium, i.e., the *transmission*. This is an ill-posed problem, since there are two unknown values for each pixel. Thus, many methods in the literature use techniques, such as multiple images,[1,2] polarization,[3,4] or special devices[5,6] to deal with this problem. However, there are many applications where only a single image is available.

The literature assumes some prior information to deal with the single image restoration. These priors help to find a transmission and/or the veiling light allowing the solution of the

Digital Object Identifier 10.1109/MCG.2018.2881388
Date of current version 6 March 2019.

Figure 1. Failure case of dehazing algorithms applied to a haze image (left side). The DCP[7] (center image) presents limitation when applied to color changes or excessive amount of noise. The proposed algorithm (right side) is able to deal with this condition.

ill-posed model. Most of these restoration algorithms are developed to deal with a specific participating medium. They lead to impressive results, e.g., the *dark channel prior* (DCP)[7] and the work presented by Fattal[8] using haze images, or the method of Ancuti *et al.*[9] and Drews *et al.*[10] using underwater images. However, a simple change in the light source, or sometimes in the structure of the imaged scene, can make those methods fail, as shown in the Figure 1.

We believe that a more general medium characteristic estimation is required to obtain a robust method to deal with environmental changes. In this context, we propose an automatic single image restoration method designed to deal with images acquired in *participating media*, mainly underwater and hazy environments. We obtain generality by using (i) a physical model, (ii) a robust estimation of the medium parameters, and (iii) a fusion of complementary *novel* priors. These characteristics enable us to successfully restore both hazy and underwater images.

Finally, we highlight the following contributions of this paper: *(i)* a new general color prior to be adopted in participating medium named *veil difference prior* (VDP) that can be interestingly seen as a generalization of the DCP[7] for participating medium; *(ii)* we also proposed a novel contrast prior based on the physical model called *contrast prior* (CP); *(iii)* a fusion strategy to estimate the transmission showing that it allows to obtain a better transmission estimation; *(iv)* results are validated in quantitative terms. Differently from the state-of-the-art that uses qualitative or quantitative evaluation based on empirical metrics, we use a dataset acquired in a controlled underwater environment where the amount of degradation is previously known.

IMAGE FORMATION MODEL

The lights propagating through a participating medium suffer from *scattering* and *absorption*. The image *signal*, i.e., the imaged scene is deteriorated by the *attenuation* where just a small portion of the light reaches the camera. Mainly, two phenomena can occur. A common one called *Forward scattering* occurs when the light rays coming from the scene are scattered in small angles. It creates a blurry effect on the image, mainly underwater. However, this effect presents a small contribution to the degradation and is frequently neglected.[4] The second phenomena, called *backscattering* results from the interaction between the illumination sources and particles dispersed in the medium. It creates a characteristic veil on the image, which reduces the contrast and attenuates the signal information.

An image captured in a participating medium can be defined for each color channel as:

$$I(x) = E_d(x) + E_{bs}(x) \tag{1}$$

where $E_d(x)$ is the direct component (signal) and $E_{bs}(x)$ is the backscattering component.

The direct component $E_d(x)$ is defined as:

$$E_d(x) = J(x)e^{-cd(x)} \tag{2}$$

where $J(x)$ is the signal with no degradation, which is attenuated by $e^{-cd(x)}$, named as transmission $t(x)$, c is the attenuation coefficient associated with the wavelength, and $d(x)$ is the distance between scene and the sensor. Considering an image taken from a Lambertian surface, $J(x)$ can also be described by the color

Published by the IEEE Computer Society IEEE Computer Graphics and Applications

constancy image formation model.[11] Omitting the camera parameters and considering the light source as constant, we have:

$$J(x) = LM(x) \tag{3}$$

where L is the light source, $M(x)$ is the reflectivity of the imaged surface.

We also consider that natural light comes from a limited cone above the scene, the optical manhole cone.[12] For this reason, we assume that the light source is related to the cone size and also influenced by the environment. Following the model proposed by Jaffe-McGlamery[13,14] and the simplification proposed by Schechner and Karpel,[4] the backscattering component, $E_{bs}(x)$, can be defined as:

$$E_{bs}(x) = A^D(1 - t(x)) \tag{4}$$

where A^D is the veiling light, here also called ambient light constant, represents the color and radiance characteristics of the medium, and D is the height between the line of sight (LOS) and the light source, e.g., the water column for underwater images. This constant is related to the *optical manhole* cone placed above the LOS. Also, the veiling light is associated with the distance between the light source and scene (d) and influenced by the environment. The term $(1 - t(x))$ weights the effect of the *backscattering* as a function of the distance, $d(x)$, from the object to the camera.

Assuming a large distance between the light source and a small variation in the height D, we can consider the LOS and the objects are all illuminated by the same light source. Thus, the ambient light, A^D, and the constant light source, L, can be approximated by the same constant. Equations (2) and (3) allow us to define the final model as:

$$I(x) = A^D M(x)t(x) + A^D(1 - t(x)). \tag{5}$$

This equation is a generalization from the *Koschmieder*[15] equation that is commonly adopted by dehazing methods such as the DCP[7] and the method of Fattal.[16] Assuming intensity values in the interval [0; 1], (5) turns into the *Koschmieder* equation when $A^D \approx [1; 1; 1]$ for the RGB representation, i.e., approximately white. All of these equations are valid for each color channer $\lambda \epsilon \{r, g, b\}$. We can jointly obtain color recovering and haze removal using (5) as detailed in the Experimental Evaluation section.

RELATED WORKS

Both the transmission and ambient light must be estimated to obtain the true object color reflectively. For this, we need to assume some properties that a haze-free image, i.e., an image without ambient interference, should have. These properties are usually image priors, or assumptions that can be used to find turbidity indicators in an image.

In the work presented by Fattal *et al.*,[16] it is assumed that there is no covariance between the reflectance and the illumination. Thus, the transmission can be defined as the source of covariance. However, Fattal *et al.*[8] showed that this assumption only works for low degradation.

Fattal *et al.*[8] also proposed a method to estimate the transmission using a *color line assumption*.[17] It infers the transmission by finding the intersection point between the color line and the vector with the orientation of the veiling light. However, the success of the method depends on various aspects. It needs to find patches were the pixels must support a line in $\mathbb{R}^3$, the patch is not an edge, the reflectance is positive when decomposed using the proposed model, the intersection angle between the line that represents the patch and the estimated air light is sufficiently large, the intersection point with the air light must be close to others intersection points, the estimated transmission must lie in the interval [0;1] and the shading must vary sufficiently. Thus, the method depends on many conditions that not always hold true in a typical situation.

One of the most important methods is based on the DCP.[7] In this method, the minimum value of the image channels in a small patch provides a transmission indication, $t(x)$. The method obtains good results, but it works only for white colored haze and does not work well for underwater environments accordantly to the work presented by Drews *et al.*[19] This method has been adapted several times for underwater environments.[10,19–22] However, all adaptations lack to consider the large range of colors that exist in an underwater environment by assuming some specific conditions such as the blue channel

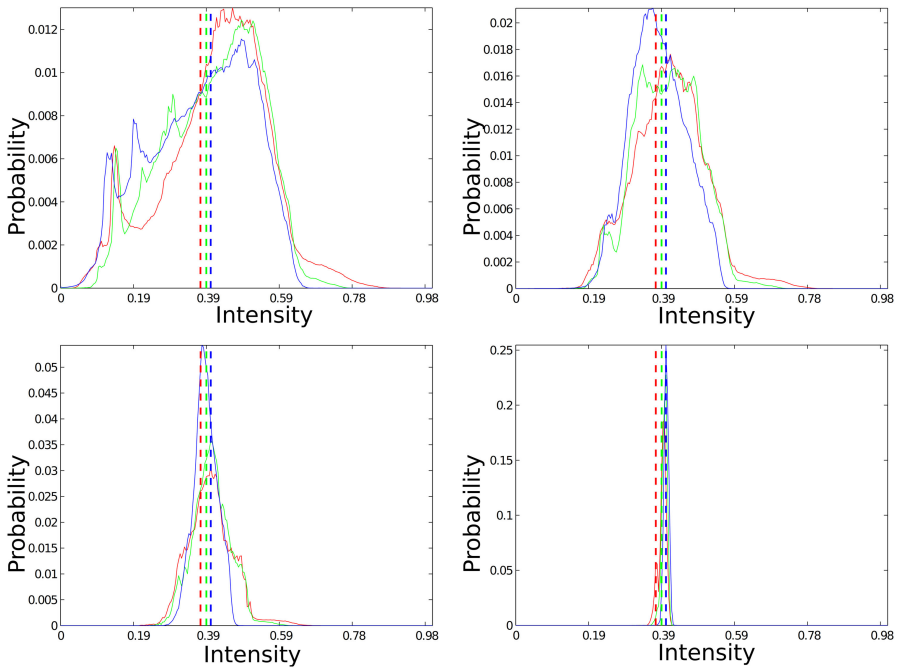

Figure 2. Histograms of a controlled underwater scene captured under several levels of degradation. T0 is an image acquired in a clean water (top left). T5 (top right), T11 (bottom left), and T20 (bottom right) present three levels of degradation created through the addition of milk on the water.[28] The ambient light is represented by the dashed lines. The color of the lines represents the three RGB channels of the images. Figure 7 shows the images adopted to obtain the histograms.

predominance[19] or the red channel absorption.[10,21] Our method does not consider that the participating media has properties such as a single color. It shows that having this assumption is helpful to obtain a general method that does not depend on which participating media we are working with. Thus, we can have a more robust method to deal with several kinds of degradation.

Recently, Ancuti *et al.*[23] introduced also a preprocessing step allowing us to apply the DCP on underwater images leading to impressive results. However, to have this method working properly is necessary to determine previously the channel that must be compensated before the white balance. As previously mentioned, our method does not make any assumption about color properties.

There are also approaches that directly manipulate some image properties, e.g., contrast, blur, and noise, in order to improve the image quality. Many general image enhancing methods can be used to recover the visibility through turbid media such as the well known CLAHE[24] and Color Constancy.[11] There are also some enhancement method based on fusion.[9,25] Although these techniques can reduce the haze leading in apparently good results, the direct manipulation of the image properties can also degrade some important properties. Moreover, enhancement methods do not usually consider the depth variation that exists in images acquired in participating media. On the other hand, the work presented by Ancuti *et al.*[26] consider the depth variation and achieves great results at the cost of needing a reference image and the attenuation map which in underwater conditions it is based on the blue or red channel.

COMPOSITE TRANSMISSION ESTIMATION

The use of a single indicator, such as the color,[7–19] or the contrast,[27] is decisive but not sufficient for most situations. For instance, it is not possible to know if a signal corresponds to an object reflectance of a given color, or if it presents a certain color due to the ambient light. The same problem occurs in the image contrast. It is not possible to know if an image area

Published by the IEEE Computer Society IEEE Computer Graphics and Applications

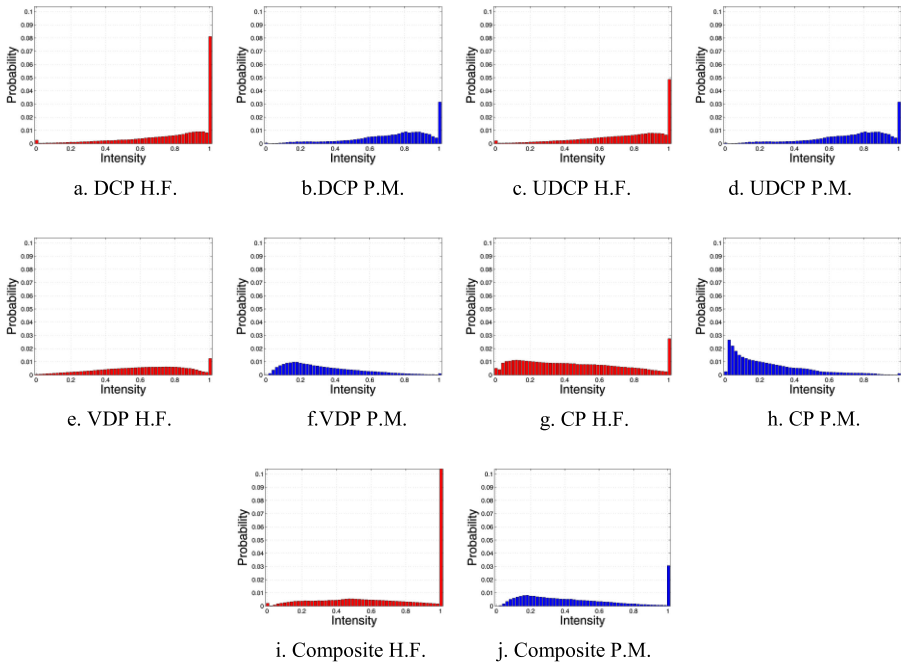

Figure 3. Average histograms for DCP,[7] UDCP,[18] VDP, CP, and Composite Prior. For haze-free (H.F.), dataset we used 2000 images from the test set of the popular ImageNet,[30] in red. For participating media (P.M.), we built a dataset by collecting 2000 images over the web using blue. The images were resized into a maximum side of 1024 pixels and the priors were computed over patches of 15 ×15 pixels. For a better understanding of results, we show sampling of the 256-bins histograms on every five bins. Also for an easier comparison we plotted 1 – DCP and also 1 – UDCP, instead of its original version. In this evaluation, the target behavior is a high response for the haze-free dataset and a lower response for participating media dataset.

presents weak contrast or if this contrast is already attenuated by the medium. Thus, we propose the *Composite Transmission* by fusing two novel image priors, the *VDP* and the *CP*.

Veil Difference Prior

Based on the image formation model observation, we stated the following assumption: the image pixel color tends to be closer to the ambient light constant when the image is degraded by the participating medium. Figure 2 shows the histogram of a controlled underwater scene imaged under several levels of degradation. It can be seen that the intensities of the pixels tend to be closer to the ambient light constant (represented by dashed lines) as the level of degradation increases. Equation (5) shows that the image pixel color tends to the ambient light constant with the increase of the optical depth (cd). We assume all pixels from a small patch $\Omega(x)$ centered at x are equally distanced to the camera. This assumption is only valid when the distance to the camera is usually larger than the distance between objects in the scene. Since it is not always valid, we estimate only a rough transmission using the veil difference as:

$$\widetilde{t_v}(x) = \frac{\max_{\lambda\in\{r,g,b\}}\left(\max_{y\in\Omega(x)}\left(\left|I_\lambda(y) - A_\lambda^D\right|\right)\right)}{\max_{\lambda\in\{r,g,b\}}\left(\max_{y\in\Omega(x)}\left(\left|J_\lambda(y) - A_\lambda^D\right|\right)\right)}. \tag{6}$$

We take the channel with the highest difference since it is the one with more information. The problem is that the haze-free image is usually unknown. On the other hand, we observe that they tend to have a significant difference to the light source on at least one of its color channels when looking at haze-free images. Formally, for an image J_λ, we define the VDP as:

$$\begin{aligned}&\max_{\lambda\in\{r,g,b\}}\left(\max_{y\in\Omega(x)}\left|J_\lambda(y) - A_\lambda^D\right|\right)\\ &= \max_{\lambda\in\{r,g,b\}}\left(\max\left(1 - A_\lambda^D, A_\lambda^D\right)\right).\end{aligned} \tag{7}$$

We compute the average histogram and other priors on 2000 haze-free images [see Figure 3(e)] and other 2000 images acquired in participating

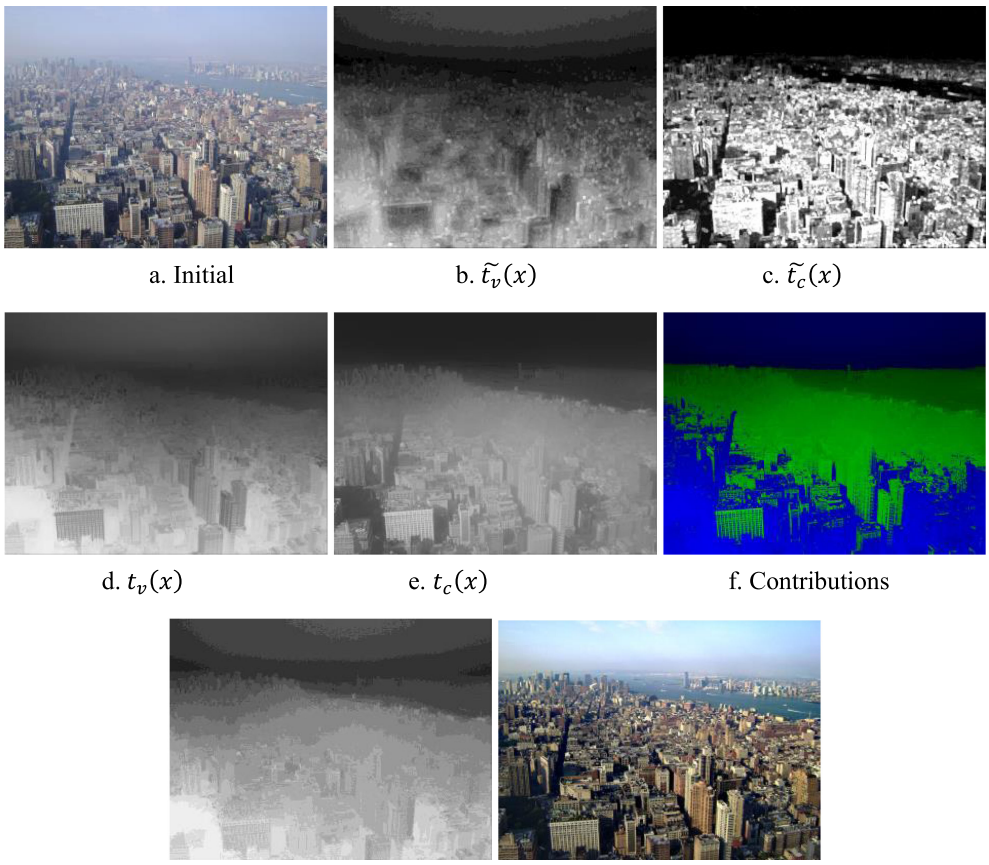

Figure 4. Result obtained by each step of the proposed method for a sample image. *Contributions* of each transmission map is obtained after the *max* operator (Eq. 13), where green represents the larger value is $t_c(x)$ or the larger transmission is $t_v(x)$, in blue.

media [see Figure 3(f)] to evaluate this prior. The result shows the prior is clearly not as strong as presented by He *et al.*[7] for haze-free images. However, the average for the prior on degraded participating media showed a soaring range of values indicating sensitivity to the presence of the medium.

Finally, the VDP can be understood as a *generalization* of the DCP presented by He *et al.*[7] Equation (7) turns into $\max(\max(1 - J_\lambda(x))) = 1$ for $\lambda \epsilon \{r, g, b\}$ which is equivalent to the DCP by assuming the ambient light color as pure white where the $A_\lambda^D = [1, 1, 1]$.

We can compute the transmission by replacing (7) by (6) using the VDP:

$$\widetilde{t_v}(x) = \frac{\max_{\lambda\in\{r,g,b\}}\left(\max_{y\in\Omega(x)}\left(\left|I_\lambda(y) - A_\lambda^D\right|\right)\right)}{\max_{\lambda\in\{r,g,b\}}\left(\max\left(1 - A_\lambda^D, A_\lambda^D\right)\right)}. \tag{8}$$

We show Veil Difference Transmission on Figure 4(b). We can notice this transmission captures the depth variation on the image.

Contrast Prior

We can observe on Figure 2 that besides the color approximation to veiling light, we have shrinking into the histogram shape, dramatically reducing the global image contrast. Thus, we assume the following local indicator: for a given image patch I_λ, the contrast on this patch tends to reduce proportionally to an increase at the presence of the medium. Thus, the contrast transmission can be computed as:

$$\widetilde{t_c}(x) = \frac{\max_{\lambda\in\{r,g,b\}}\left(\max_{y\in\Omega(x)}(I_\lambda(y)) - \min_{y\in\Omega(x)}(I_\lambda(y))\right)}{\max_{\lambda\in\{r,g,b\}}\left(\max_{y\in\Omega(x)}(J_\lambda(y)) - \min_{y\in\Omega(x)}(J_\lambda(y))\right)} \tag{9}$$

this ratio, analogously to (9), represents the lost of contrast information due to the medium.

Published by the IEEE Computer Society IEEE Computer Graphics and Applications

However, the contrast of the haze-free version of image is not available. So, we assume that haze-free image patches present the maximum possible range defining the CP as:

$$\max_{\lambda\in\{r,g,b\}}\left(\max_{y\in\Omega(x)}(J_\lambda(y))-\min_{y\in\Omega(x)}(J_\lambda(y))\right)=1. \quad (10)$$

For the CP, we also made a statistical evaluation on a large dataset that can be seem in Figure 3. The Figure 3(g) shows that a significant number of patches have value one. Also, it presents a similar behavior as the VDP and UDCP [see Figure 3(h)]. Thus, we have the contrast transmission computed as:

$$\widetilde{t_c}=\max_{\lambda\in\{r,g,b\}}\left(\max_{y\in\Omega(x)}(I_\lambda(y))-\min_{y\in\Omega(x)}(I_\lambda(y))\right). \quad (11)$$

We show the contrast transmission on Figure 4(c). We can observe that this transmission is sparse but presents also the depth variation.

Refining Transmission

When the transmission is computed over a patch, $\Omega(x)$, it produces a coarse estimation. Then, the transmission map for $\tilde{t}_v(x)$ and $\tilde{t}_c(x)$ must be refined. For this, we chose to use the soft matting algorithm.[29]

Many other refinement algorithms have been applied with smaller computational costs.[8–21] However, the algorithm proposed by Levin *et al.*[29] not solely maximizes the agreement of the transmission with edges and corners of the image. Also, it tends to spread the transmission when there is discontinuities in the rough transmission $\tilde{t}$. This maximization is especially effective when there is more sparse measures such as the CP [see Figure 4(c) and (e)].

Composite Transmission

We state that the transmission can be computed by joining multiple priors by the function:

$$t(x)=f(t_1(x),t_2(x),\ldots,t_n(x)). \quad (12)$$

In this paper, we assume a conservative function. We consider that, when a pixel presents a high transmission value, this indication is usually related to the information of the signal and unrelated to the veiling. Thus, we propose a simple combination of transmission estimators by using a max function. We denote the transmission of a pixel x as:

$$t(x)=\max(t_v(x),t_c(x)) \quad (13)$$

where $t_v(x)$ is the refined transmission computed with the *VDP* and $t_c(x)$ is the refined transmission computed with the *CP*. We also show the statistical analysis for the *Composite Transmission*, arguably to be the most reliable behavior. For haze-free images [see Figure 3(i)], there is a clear tendency of assuming the value one than only the VDP. It combines the better of two worlds, having high range of values for participating media images and a solid high response for haze-free images. This corroborates to obtain the generality of the proposed method.

We also show on Figure 4(f) the contribution from each of the image priors after applying the Equation (13). We notice that the intermediate range transmissions are dominated by the contrast transmission. The final transmission is shown in Figure 4(g).

Restoration

The image with restored visibility [see Figure 4(h)] is obtained by isolating the object reflectivity $M(x)$ on (5) for each color channel λ:

$$M(x)=\frac{I(x)-A^D+A^Dt(x)}{\max(t_0,A^Dt(x))} \quad (14)$$

where t_0 parameter is a minimum transmission. This parameter avoids restoring noise when there is no information behind the veil. Typical values range between [0.1, 0.2].

Estimating the Ambient Light

Several authors estimate the ambient light as the brightest pixels in the image such as the works presented by Tan *et al.*[27] and Fattal *et al.*[16] This estimation presents some drawbacks, especially if the ambient light is not present on the image. The work presented by Sulami[31] proposes a method that divides the estimation into orientation and magnitude and does not need the presence of an ambient light pixel on the image. However, it depends on finding patches that obey certain properties.

As we stated in the Image Formation Model section, the ambient light is associated with the light source on the scene. Thus, it is reasonable

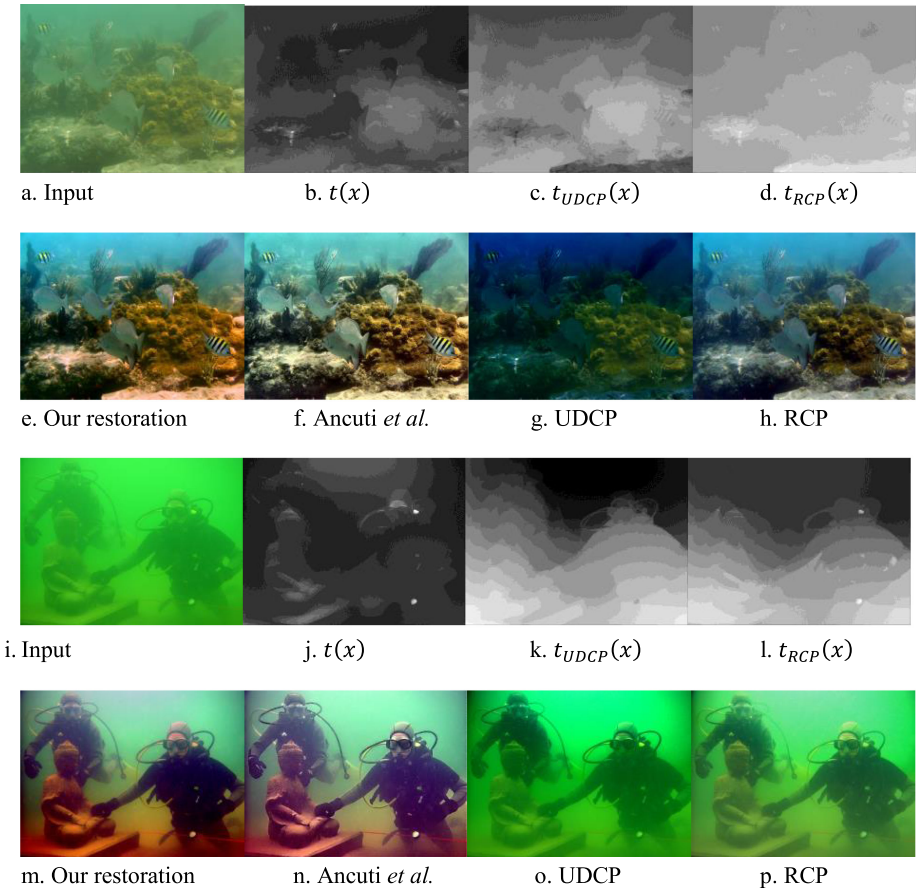

Figure 5. Restoration obtained by our method and the methods RCP, UDCP, and Ancuti *et al.*[9] and its associated transmission. The underwater input images acquired by Ancuti *et al.*[9] that do not provide the transmission.

to use color constancy techniques, commonly adopted to find the light source color on general images. Techniques such as gray edge,[11] the gray world, the max-rgb or the shades-of-gray[32] can be used. The problem of the gray edge technique is the edges are normally blurry and the gray world technique fails when there are too many close objects. Max-rgb is dependent on white patches fully reflecting the light information. We find the shades-of-gray algorithm encapsulates the best behavior for participating medium. The algorithm obtains estimation in between the average of the scene and the reflectivity of a white patch.

EXPERIMENTAL EVALUATION

Experimental results are obtained by a standard C++ with OpenCV library. All the parameters are defined as explained on previous sections. We compared the results with state-of-the-art methods. For most of the cases, we adopted the provided images by the authors to reproduce their results. The estimation of the transmission using Red Channel (RCP)[21] and DCP[7] were implemented according to the paper by using also a standard C++ with OpenCV. UDCP[10,18] results are obtained using the source code provided by the authors.

Qualitative Evaluation

Figure 5 shows the results obtained for the underwater environment. The proposed method tends to not overestimate transmission. This result is mainly due to the observation that the ambient light color is not necessarily present on the image. The RCP assumption works quite well for Figure 5(a) with a small overestimation. However, red channel method clearly presents

Published by the IEEE Computer Society IEEE Computer Graphics and Applications

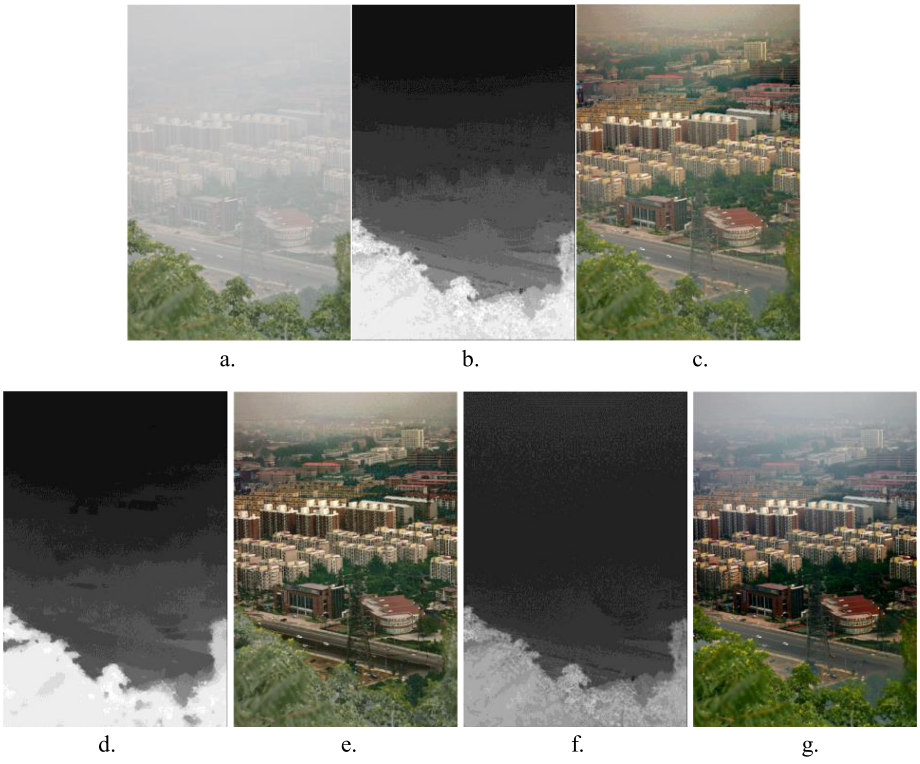

Figure 6. Results for a haze image restoration: (a) input image; (b) transmission using DCP; (c) restoration using DCP; (d) transmission by Fattal;[8] (e) restoration obtained by Fattal;[8] (f) our transmission; (g) our restoration.

Figure 7. Samples of the TURBID dataset collected by Duarte *et al.*[28]

problems by overestimating transmission on red objects with high amount of degradation [e.g., in Figure 5(p)].

There is a clear tendency of our method to present more contrasted colors and less noise, but with slightly less contrast when comparing the results with the work presented by Ancuti *et al.*[9] [see Figure 5(c) and (h)]. It is due to the use of optical model of the participating media. Our method is capable to recover color proper- ties without further use of white balances and compensations. This can be seen when comparing the proposed method with the UDCP,[10,18] where a good restoration is obtained [see Figure 5 (d)] but with an unsatisfactory color correction.

As stated earlier, our method is designed to restore multiple types of participating media without any parameter adjustment. In Figure 6, we show the results of our method on a haze image comparing with other state-of-the-art methods. We assume the ambient light is not a pixel from the scene. It helps to avoid the over-estimation of the transmission on lower distances. However, due the max operation between the priors on longer distances our method culminates into overestimating the transmission. Finally, we also see a better color correction when compared to the results presented by the Fattal's[8] work and DCP. We explain this color enhancement due to the assumption that the haze is not perfectly white.

Table 1. Quantitative evaluation of the proposed method using images from Middleburry portion of the D-HAZE dataset.[33] For each image, we show SSIM/CIEDE2000 indexes between ground truth and the method output. The indexes for DCP,[7] Meng *et al.*,[36] Fattal,[16] Ancuti and Ancuti,[37] Tarel,[35] and CLAHE[34] are those provided by Ancuti *et al.*[33] We provided also average and standard deviation for all evaluated images. The top-3 highest scores for each index are presented in green, blue, and red, respectively.

	Our Method	CLAHE	Tarel	Ancuti and Ancuti	DCP	Meng *et al.*	Fattal
Adirondack	0.75/16.33	0.73/11.26	0.85/15.19	0.89/10.82	0.86/10.77	0.88/11.11	0.75/16.06
Backpack	0.81/14.21	0.61/14.90	0.87/11.72	0.88/11.74	0.92/10.01	0.89/10.63	0.87/13.30
Bicycle1	0.77/12.97	0.77/18.07	0.89/8.84	0.90/12.67	0.88/15.30	0.77/23.26	0.81/16.45
Cable	0.65/20.55	0.50/25.05	0.65/26.47	0.62/24.25	0.71/16.38	0.67/18.89	0.74/13.68
Classroom1	0.83/16.48	0.61/11.20	0.80/23.31	0.89/11.84	0.91/6.31	0.87/9.83	0.87/20.74
Couch	0.78/11.45	0.61/11.52	0.72/25.64	0.85/13.26	0.91/6.74	0.86/10.77	0.78/22.94
Flowers	0.77/18.71	0.70/16.91	0.79/15.86	0.82/14.62	0.88/8.65	0.83/14.01	0.88/8.70
Jadeplant	0.72/27.11	0.55/26.36	0.69/20.19	0.63/28.41	0.69/19.22	0.70/21.42	0.63/32.39
Mask	0.79/13.33	0.68/14.78	0.87/11.75	0.86/11.60	0.89/9.70	0.83/14.87	0.89/11.82
Motorcycle	0.66/22.33	0.76/13.03	0.76/18.58	0.82/14.49	0.82/13.71	0.80/14.10	0.76/17.86
Piano	0.73/9.05	0.70/9.76	0.79/20.30	0.84/10.34	0.89/6.18	0.85/8.86	0.79/12.59
Pipes	0.62/16.93	0.63/16.90	0.68/24.28	0.71/19.19	0.78/9.64	0.75/11.54	0.68/15.46
Playroom	0.75/12.14	0.67/11.95	0.79/18.37	0.83/13.23	0.88/7.43	0.82/12.07	0.80/16.09
Playtable	0.72/14.43	0.72/9.42	0.83/19.06	0.84/9.12	0.91/8.03	0.86/14.12	0.81/11.52
Recycle	0.74/21.92	0.69/13.4	0.89/11.89	0.90/12.47	0.88/14.96	0.87/14.85	0.73/20.65
Shelves	0.82/14.58	0.75/7.68	0.88/15.20	0.93/7.18	0.89/11.65	0.89/14.41	0.87/12.40
Shopvac	0.68/19.46	0.67/17.66	0.73/29.25	0.79/19.27	0.83/16.29	0.82/17.57	0.76/32.50
Sticks	0.84/15.67	0.71/20.07	0.88/8.49	0.85/15.21	0.95/7.21	0.95/8.20	0.92/10.86
Storage	0.71/19.99	0.69/13.33	0.85/16.64	0.81/14.78	0.88/10.19	0.87/12.09	0.82/16.85
Sword1	0.80/13.39	0.61/20.07	0.86/12.10	0.83/14.81	0.91/9.66	0.89/10.44	0.86/13.82
Sword2	0.80/23.08	0.64/12.18	0.87/13.48	0.89/12.05	0.90/12.46	0.85/15.49	0.76/37.96
Umbrella	0.86/16.22	0.57/20.37	0.82/15.13	0.84/15.93	0.84/20.23	0.80/21.49	0.66/33.15
Vintage	0.85/17.66	0.71/14.91	0.86/8.24	0.86/14.61	0.92/10.05	0.78/21.80	0.86/15.79
Average	0.76/16.87	0.66/15.25	0.81/16.96	0.83/14.43	0.86/11.34	0.83/14.43	0.80/18.42
Std.Dev.	0.07/4.30	0.07/4.82	0.07/5.96	0.08/4.71	0.064/4.07	0.07/4.41	0.08/8.09

Quantitative Evaluation

The literature usually compares the methods using a qualitative perception of image quality. However, it is hard to evaluate which is the best restored image, e.g the Figure 5(c) and (b).

An effective way to evaluate dehazing algorithms quality is by comparing them with a ground truth image, i.e., a version of the image without the effects of the medium. For this, we adopted the TURBID dataset collected by Duarte *et al.*[28] They reproduced a scene of an underwater environment where multiple images are captured with an increasing degradation by the addition of milk. The Figure 7 shows four image samples of the TURBID dataset.

Also, in order to evaluate our method for haze images we used the D-Haze dataset.[33] This dataset is composed of images with synthetic haze. Table 1 shows that our method performs reasonably well for haze images, obtaining better SSIM than CLAHE[34] and better CIEDE2000 than Tarel[35] and Fattal.[16]

We show in Figure 8 the mean square error in function of the quantity of milk that is related

Published by the IEEE Computer Society IEEE Computer Graphics and Applications

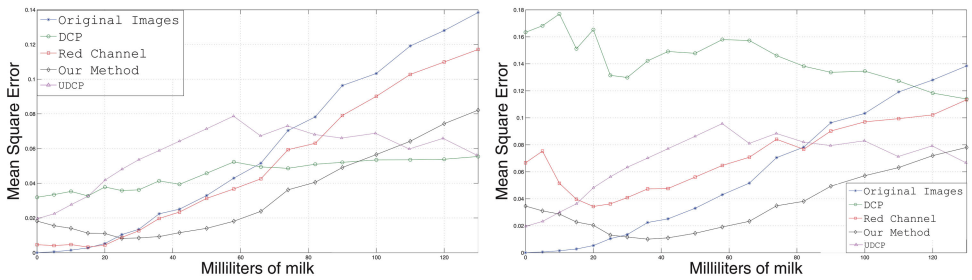

Figure 8. Quantitative evaluation of the proposed method using the TURBID dataset. The curves represent the MSE in function of quantity of milk. Each degraded image is compared with the clean image (Figure 7(a)).

with the degradation produced by the participating medium. The error is measured based on the difference between the restored image and the clean image (no milk). We compare our result with the state-of-the-art methods such as RCP, DCP, and UDCP and also the degraded images (original images), i.e., without any kind of restoration. The blue line presents the error obtained using the degraded images. Based on the error of the degraded image, our method performs an effective restoration since the image becomes closer to the ground truth.

The ambient light constant remains the same in Figure 8(a) where the proposed method achieved the lowest average error. However, it has a higher error than DCP and UDCP on strongly degraded images. In Figure 8(b), each method estimates its own ambient light constant. The proposed method performed better when compared with other methods since the ambient light constant estimated by DCP and the RCP are not accurate.

CONCLUSION

In this paper, we proposed a novel automatic single image restoration method to restore images captured in participating media. The method is inspired by the insufficiency of single priors restoration and their lack of generality for use in multiple environments. We proposed two novel priors to be used in a larger variety of environments and a way to robustly integrate them. These priors and the image formation model produce an algorithm to be used on a large range of environment conditions. This generality is one of the main contributions of this paper.

We evaluated the proposed method in several kinds of participating medium obtaining competitive results related with the state-of-the-art. Finally, we also evaluated our method quantitatively by using the TURBID dataset. We observed that the proposed method is able to restore images in a larger range of degradation conditions. Finally, as a future work, we intend to assess several strategies to fuse transmission priors, and incorporate other source of information in our transmission estimation.

ACKNOWLEDGMENTS

The authors would like to thank the Brazilian Petroleum Corporation - Petrobrás, the Brazilian National Agency of Petroleum, Natural Gas and Biofuels (ANP), to the Funding Authority for Studies and Projects and to Ministry of Science and Technology (MCT) for their financial support through the Human Resources Program of ANP to the Petroleum and Gas Sector - PRH-ANP/MCT. This paper is also a contribution of the Brazilian National Institute of Science and Technology - INCT-Mar COI funded by CNPq Grant 610012/2011-8.

REFERENCES

1. M. Roser, M. Dunbabin, and A. Geiger, "Simultaneous underwater visibility assessment, enhancement and improved stereo," in *Proc. IEEE Int. Conf. Robot. Automat.*, 2014, pp. 3840–3847.
2. P. Drews-Jr, E. R. Nascimento, M. F. M. Campos, and A. Elfes, "Automatic restoration of underwater monocular sequences of images," in *Proc. IEEE/RSJ Int. Conf. Intell. Robots Syst.*, 2014, pp. 1058–1064.

3. Y. Schechner, S. Narasimhan, and S. Nayar, "Polarization-based vision through haze," *Appl. Opt.*, vol. 42, no. 3, pp. 511–525, 2003.
4. Y. Schechner and N. Karpel, "Recovery of underwater visibility and structure by polarization analysis," *IEEE J. Ocean. Eng.*, vol. 30, no. 3, pp. 570–587, Jul. 2005.
5. S. Narasimhan, S. Nayar, B. Sun, and S. Koppal, "Structured light in scattering media," in *Proc. IEEE Int. Conf. Comput. Vis.*, 2005, pp. 420–427.
6. C. Fuchs, M. Heinz, M. Levoy, H.-P. Seidel, and H. Lensch, "Combining confocal imaging and descattering," *Comput. Graph. Forum*, vol. 27, no. 4, pp. 1245–1253, 2008.
7. K. He, J. Sun, and X. Tang, "Single image haze removal using dark channel prior," *IEEE Trans. Pattern Anal. Mach. Intell.*, vol. 33, no. 12, pp. 2341–2353, Dec. 2011.
8. R. Fattal, "Dehazing using color-lines," *ACM Trans. Graph.*, vol. 34, no. 1, 2014, Art. no. 13.
9. C. Ancuti, C. O. Ancuti, T. Haber, and P. Bekaert, "Enhancing underwater images and videos by fusion," in *Proc. IEEE Conf. Comput. Vis. Pattern Recognit.*, 2012, pp. 81–88.
10. P. L. J. Drews-Jr, E. R. Nascimento, S. S. C. Botelho, and M. F. M. Campos, "Underwater depth estimation and image restoration based on single images," *IEEE Comput. Graph. Appl.*, vol. 36, no. 2, pp. 24–35, Mar./Apr. 2016.
11. J. Van De Weijer, T. Gevers, and A. Gijsenij, "Edge-based color constancy," *IEEE Trans. Image Process.*, vol. 16, no. 9, pp. 2207–2214, Sep. 2007.
12. T. Cronin and N. Shashar, "The linearly polarized light field in clear, tropical marine waters: Spatial and temporal variation of light intensity, degree of polarization and e-vector angle," *J. Exp. Biol.*, vol. 204, no. 14, pp. 2461–2467, 2001.
13. J. S. Jaffe, "Computer modeling and the design of optimal underwater imaging systems," *IEEE J. Ocean. Eng.*, vol. 15, no. 2, pp. 101–111, Apr. 1990.
14. B. L. McGlamery, "A computer model for underwater camera systems," *Proc. SPIE*, vol. 0208, pp. 221–231, 1980.
15. H. Koschmeider, "Theorie der horizontalen sichtweite," *Beitr. Phys. FreienAtm.*, vol. 12, pp. 171–181, 1990.
16. R. Fattal, "Single image dehazing," *ACM Trans. Graph.*, vol. 27, no. 3, 2008, Art. no. 72.
17. I. Omer and M. Werman, "Color lines: Image specific color representation," in *Proc. IEEE Comput. Vis. Pattern Recognit.*, 2004, vol. 2, pp. II–II.
18. P. Drews-Jr, E. Nascimento, F. Codevilla, S. Botelho, and M. Campos, "Transmission estimation in underwater single images," in *Proc. IEEE Int. Conf. Comput. Vis. Workshops*, 2013, pp. 825–830.
19. J. Y. Chiang and Y. Chen, "Underwater image enhancement by wavelength compensation and dehazing," *IEEE Trans. Image Process.*, vol. 21, no. 4, pp. 1756–1769, Apr. 2012.
20. F. M. Codevilla, S. S. C. Botelho, P. L. J. Drews-Jr, N. Duarte Filho, and J. F. Gaya, "Underwater single image restoration using dark channel prior," in *Proc. Symp. Automat. Comput. Naval, Offshore Subsea*, 2014, pp. 18–21.
21. A. Galdran, D. Pardo, A. Picón, and A. Alvarez-Gila, "Automatic redchannel underwater image restoration," *J. Visual Commun. Image Represent.*, vol. 26, pp. 132–145, 2015.
22. H. Lu, Y. Li, L. Zhang, and S. Serikawa, "Contrast enhancement for images in turbid water," *J. Opt. Soc. Amer. A*, vol. 32, no. 5, pp. 886–893, 2015.
23. C. O. Ancuti, C. Ancuti, C. De Vleeschouwer, and P. Bekaert, "Color balance and fusion for underwater image enhancement," *IEEE Trans. Image Process.*, vol. 27, no. 1, pp. 379–393, Jan. 2018.
24. R. Hummel, "Image enhancement by histogram transformation," *Comput. Graph. Image Process.*, vol. 6, no. 2, pp. 184–195, 1977.
25. S. Bazeille, I. Quidu, L. Jaulin, and J. Malkasse, "Automatic underwater image pre-processing," in *Proc. Caracterisation du Milieu Marin*, 2006, pp. 1–8.
26. C. O. Ancuti, C. Ancuti, C. D. Vleeschouwer, and R. Garcia, "Locally adaptive color correction for underwater image dehazing and matching," in *Proc. IEEE Conf. Comput. Vis. Pattern Recognit. Workshops*, Jul. 2017, pp. 997–1005.
27. R. T. Tan, "Visibility in bad weather from a single image," in *Proc. IEEE Conf. Comput. Vis. Pattern Recognit.*, 2008, pp. 1–8.
28. A. Duarte, F. Codevilla, J. O. Gaya, and S. S. Botelho, "A dataset to evaluate underwater image restoration methods," in *Proc. OCEANS 2016 - Shanghai*, 2016, pp. 1–6.
29. A. Levin, D. Lischinski, and Y. Weiss, "A closed-form solution to natural image matting," *IEEE Trans. Pattern Anal. Mach. Intell.*, vol. 30, no. 2, pp. 228–242, Feb. 2008.
30. O. Russakovsky *et al.* "ImageNet large scale visual recognition challenge," *Int. J. Comput. Vis.*, vol. 115, pp. 1–42, 2015.

31. M. Sulami, I. Geltzer, R. Fattal, and M. Werman, "Automatic recovery of the atmospheric light in hazy images," in *Proc. IEEE Int. Conf. Comput. Photogr.*, 2014, pp. 1–11.
32. G. D. Finlayson and E. Trezzi, "Shades of gray and colour constancy," in *Proc. IS&T CIC*, 2004, pp. 37–41.
33. C. Ancuti, C. O. Ancuti, and C. De Vleeschouwer, "D-hazy: A dataset to evaluate quantitatively dehazing algorithms," in *Proc. IEEE Int. Conf. Image Process.*, Sep. 2016, pp. 2226–2230.
34. K. Zuiderveld, "Viii.5. - contrast limited adaptive histogram equalization," in *Graphics Gems*, P. S. Heckbert, Ed. New York, NY, USA: Academic, 1994, pp. 474–485.
35. J. Tarel and N. Hautiere, "Fast visibility restoration from a single color or gray level image," in *Proc. IEEE 12th Int. Conf. Comput. Vis.*, 2009, pp. 2201–2208.
36. G. Meng, Y. Wang, J. Duan, S. Xiang, and C. Pan, "Efficient image dehazing with boundary constraint and contextual regularization," in *Proc. IEEE Int. Conf. Comput. Vis.*, 2013, pp. 617–624.
37. C. O. Ancuti and C. Ancuti, "Single image dehazing by multi-scale fusion," *IEEE Trans. Image Process.*, vol. 22, no. 8, pp. 3271–3282, Aug. 2013.

Joel Felipe de Oliveira Gaya is currently working toward the Master's degree in computer engineering at the Federal University of Rio Grande (FURG), Rio Grande, Brazil, under the supervision of Prof. Silvia S.C. Botelho and Paulo Drews-Jr. He graduated in computer engineering from the FURG, in 2016. His main research interests include image processing and machine learning. Contact him at joelfelipe94@gmail.com.

Amanda Duarte is currently a Researcher with the Barcelona Supercomputing Center and working toward the Ph.D. degree at Universitat Politècnica de Catalunya, Barcelona, Spain, under the supervision of Prof. Jordi Torres and Prof. Xavier Giró. In 2015, she received the Graduate degree in systems analysis from Instituto Federal Sul-rio-grandense Câmpus Pelotas, Pelotas, Brazil, spending one year at Northern Virginia Community College in the United States as part of an exchange program. She received the Master's degree in computer engineering from Universidade Federal do Rio Grande, Rio Grande, Brazil, under the supervision of Prof. Silvia Silva da Costa Botelho and Prof. Paulo Lilles Jorge Drews Junior. Her current research interests lie in the area of computer vision, machine learning, neural machine translation, speech recognition, video generation, video understanding, and multimodal learning. Contact her at a.duarte@furg.br

Felipe Codevilla Moraes is currently working toward the Ph.D. degree at the Computer Vision Center, Barcelona, Spain. His Ph.D. focuses on machine learning and autonomous driving. He graduated and holds the Master's degrees in computer engineering from the Federal University of Rio Grande, Rio Grande, Brazil. During his Master's he did a 10-month Research Internship at the University of Girona. During his Ph.D. he was also a research intern at INTEL labs in Munich. Contact him at felipe.alcm@gmail.com.

Paulo Drews-Jr is currently an Assistant Professor with the Center for Computational Science - C3, Federal University of Rio Grande (FURG), Rio Grande, Brazil, and Vice-Chair of the IEEE South Brazil RAS Chapter. He was a researcher at the ISR Coimbra's Mobile Robotics Lab. He was also a Visiting Researcher with the Autonomous System Lab at QCAT-CSIRO, Brisbane, Australia. His main research interests are robotics, computer vision, image processing, pattern recognition, and machine learning. He graduated in computer engineering from the FURG, in 2007. He received the D.Sc. and M.Sc. degrees in computer science from Federal University of Minas Gerais, Belo Horizonte, Brazil. His doctoral dissertation was focused on restoration of images acquired in participating media. His Master's thesis was focused on change detection and shape retrieval in 3-D Maps. Contact him at paulodrews@furg.br.

Silvia Silva da Costa Botelho is a Professor with the Federal University of Rio Grande (FURG), Rio Grande, Brazil, and the Director of the Centro de Ciencias Computacionais, Rio Grande, Brazil. She is also the Founder and Director of Robotics and Intelligent Automation, FURG. She is a member of the Robotics Committee of the Brazilian Computer Society. Her research interests include automation and computer science focus on sensor grids, intelligent systems, and robotics. She received the Ph.D. degree in robotics from the Laboratoire d'Analyse et d'Architecture des Systemes, Toulouse, France. Contact her at silviacb@furg.br.